Aeolian Dynamics of Beach Scraped Ridge and Dyke Structures

Thomas A.G. Smyth[1] and Patrick A. Hesp[1]

[1] School of the Environment, Faculty of Science and Engineering, Flinders University, Bedford Park, South Australia 5042

Keywords

Beach Scraping, Foredune, Scraped and Engineered Structures, Dune Restoration, Computational Fluid Dynamics, Aeolian, Sediment Transport, Ridges, Dykes, Dune Management.

Abstract

Where urban areas are situated close to a beach, sand dunes act as protection from flooding and erosion. When a dune has been removed or damaged by erosion, dune, ridge or dyke re-building using heavy machinery, a process known as beach scraping, is a common method of restoration. Following construction, natural accretion of sediment on the backshore is preferable as it facilitates sustained natural dune building, growth of vegetation, habitat creation and reduces the need for further beach scraping.

This study investigates the near surface flow and transport potential for three artificial structure designs: a single ridge, a double ridge and a dyke. The three shapes contained an identical volume of sand and were preceded by 50 m of beach at an angle of 3°. A computational fluid dynamic model (CFD) was created for each scenario to calculate wind flow and shear velocity from 4 different wind directions at 22.5° intervals from 0° (onshore) to 67.5°. From this data sediment flux was predicted along a two dimensional transect for each of the scenarios.

For all structures, shear velocity on the beach and stoss slope decreased as incident wind direction became more oblique, conversely shear velocity in the lee of the crest increased. A reduction in shear velocity at the foot of each structure also occurred and appears related to stoss slope, with the reduction greatest reduction at the toe of the dyke structure (stoss slope 34°) and the least before the single ridge (stoss slope 17°).

Specifically the results suggest that the double ridge structure is the most resilient to aeolian erosion. Shear velocity reduction on the back beach is comparable to the dyke and sediment flux from the stoss slope of the double ridge structure may become trapped in the swale between the two ridges encouraging sediment deposition, thus reducing sediment transport beyond the dunes and backshore. Although the dyke structure underwent the greatest reduction in shear velocity on the back beach it experienced substantial sediment flux at the crest and along the top of the structure, making it susceptible to erosion during a strong wind event. The highest sediment transport rate was calculated at the crest of the single ridge, and the single ridge structure also created the smallest reduction of shear velocity on the back beach, thus making it less desirable than the double ridge.

1. *Introduction*

Foredunes, the shore-parallel sand dunes immediately landward of the active beach formed by aeolian sedimentation within plants (Hesp, 2002), are an important landform of sandy coastlines. They provide a myriad of ecosystem services (Nordstrom and Jackson, 2013) such as habitat for flora and fauna, a site of nutrient recycling and accumulation (Olff et al., 1993), recreational space, a store of sediment for storm and wave erosion, and a barrier against coastal flooding and erosion (Conaway and Wells, 2005). The foredune's effectiveness as a coastal defence is becoming increasingly valuable to coastal managers and engineers as a more sustainable and cost effective alternative to hard engineering structures, particularly as global climate is predicted to raise sea levels (IPCC, 2012) and possibly increase extreme storm frequency and intensity (Webster et al., 2005).

As sandy shorelines are highly valued for their economic and social values throughout the world, the encroachment of urban areas on the coast is a global problem (Martínez et al., 2013). Coastal dunes have been subject to erosion and removal by both natural and anthropogenic processes across the world (Gómez-Pina et al., 2002). Along urbanised coastlines, naturally occurring dunes have been removed and replaced with ocean front property, urban and industrial infrastructure, and recreational facilities (Martínez et al., 2013). Sediment transport mechanisms have been disrupted by changes to sediment budgets through the construction of dams (Willis et al., 2003), harbours, jetties, groynes (Hall and Pilkey, 1991) and sand mining, causing beach widths to recede, dunes to erode and, in some cases, disappear. Dune building and creation on the backshore has also been compromised by beach raking (Nordstrom and Jackson, 2013), trampling (Hylgaard and Liddle, 1981) and agriculture (Whitehead, 1964). Measures to protect and/or restore dunes or a protective structure on the backshore have involved erecting sand fencing to trap sediment, beach nourishment, dune or dyke construction, vegetation planting, boardwalk construction and elevating pathways to ease trampling, changes to agricultural policy, re-routing major infrastructure, visitor education, and access limitation (Gómez-Pina et al., 2002).

Where a dune has been removed or damaged, scraping the uppermost layers of sediment from the beach to rebuild the foredune is a common, immediate form of restoration (Bruun, 1983), particularly in the United States (Bruun, 1983; Petersen et al., 2000; Conaway and Wells, 2005) and Australia (Cooke et al., 2012). Small dunes or berms termed 'bankets' are also commonly constructed on the back beach in the Netherlands (Nordstrom and Arens, 1998). The process of beach scraping to create a backshore structure or dyke is performed by bulldozers or earth moving equipment which scrapes the top layer (typically 0.2 m – 0.5 m) of sand from the beach and pushes sediment into a 'dune' or other shape on the backshore or adjacent to a former dune or other landform unit (Nordstrom and Arens, 1998).

Although there is some guidance on how to build dune and artificial structures in the United States (MacArthur et al., 2005) and Australia (NSW Department of Land and Water Conservation, 2001), these guidelines are not specific to dunes or structures created by beach scraping and take no account of aeolian processes once the structure has been made. Structures created by beach scraping are vulnerable to wind erosion as they are not always vegetated following construction. Aeolian transport may lead to the rapid deflation of these structures causing 'nuisance dunes' to form in their lee (Nordstrom and Arens, 1998). Not only does removal of wind-blown sand from

urban areas have a significant cost to private property owners and municipalities (Nichols, 1996), but the removal of sediment greatly reduces the dunes or structures effectiveness as a sediment store and a barrier to coastal erosion and flooding.

This paper investigates near surface wind flow and resulting sediment transport on three scraped ridge and dyke structures commonly constructed along developed shorelines following storm erosion. Wind flow over 3 structures is simulated using a computational fluid dynamic (CFD) model and the sediment flux over each ridge/dyke structure predicted.

2. *Methodology*

2.1 Scraped Structure Design

The three structures selected were a single symmetrical or triangular-shaped ridge, a double ridge and dyke with a steep seaward riser and flat tread or crest (Figure 1). To maximise comparability of ridge/dyke shapes, each structure was a maximum of 3 metres high and had a cross sectional area of 30 m^2. The angle of the slope on both single and double triangular structures was below the angle of repose for dry sand (34°) at 17° and 31° respectively, whilst slopes of the dyke were at the angle of repose (34°) (Figure 1). A slope of 3° was chosen for the beach slope as it represents the upper range of mean beach slopes for intermediate beaches and lies within the mid-range gradient of most beaches (see table 7.1 in Short, 1999).

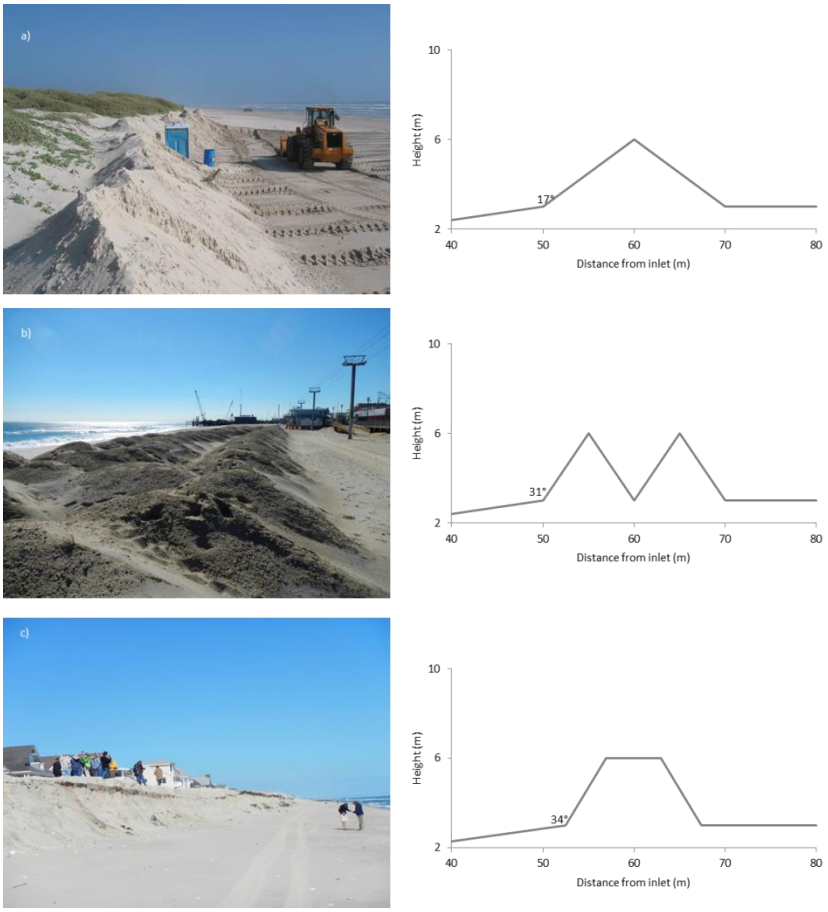

Figure 1. Left: Beach scraped structures from Texas (a) and New Jersey (b and c). Right: Simplified two dimensional structures based on field examples. The distance from the inlet refers to the

distance from the computational wind inlet. Note that there is considerable vertical exaggeration in the topographic profiles illustrated.

2.2 Dune morphological modelling

To date the majority of dune morphological modelling has been performed using cellular automaton (CA) models (Werner, 1995; Bass, 2002). Although CA modelling is effective at creating realistic dune forms under a range of conditions such as wind direction (Zhang et al., 2012) and vegetation (Nield and Baas, 2008), the simple assumptions determining the models outcome cannot yet be used to predict morphological change in reality (Zheng, 2009). Furthermore the two-dimensional nature of flow modelling conducted in CA modelling does not permit users to adequately investigate lateral patterns of deposition or erosion that may occur.

Due to these limitations a computational fluid dynamic model (CFD) was used to calculate near surface wind speed. CFD has the advantage of being able to model flow in three-dimensions and solve areas of flow separation and reversal as it considers both the conservation of momentum and the conservation of mass. This allows the investigation of wind flow patterns and resulting shear stress over complex dune topographies for a range of wind directions. It has also been validated over a range of complex dune morphologies (Wakes et al., 2010; Jackson et al., 2011; Smyth et al., 2013; Hesp et al., in press). As the CFD modelling technique employed only simulated the wind flow and did not provide any morphological feedback, potential sediment transport on the structures was calculated using shear velocity by the model of Lettau and Lettau (1977) and corrected for slope according to Bagnold (1973).

2.2.1 Computational Fluid Dynamics (CFD) model

The air flow dynamics over each structure was simulated using the computational fluid dynamics (CFD) software OpenFOAM. CFD uses numerical algorithms which integrate the governing equations of fluid flow over a domain by converting the integral equations to algebraic equations, before solving them iteratively (Versteeg and Malalasekera, 2006).

In this study, flow was calculated using Reynolds-Averaged Navier-Stokes (RANS) equations which produce an average of flow motion over time. OpenFOAM's large time-step transient solver for incompressible flow, *PIMPLE*, was used to solve the flow, and turbulence was modelled using the two-equation Re-Normalised Group (RNG) k-ε turbulence model. This turbulence model was chosen due to its good performance compared to measured data over complex dune topography (Pattanapol et al., 2007; Wakes et al., 2010; Smyth et al., 2012; 2013). Simulations were run in parallel across 40 cores on the Flinders University high performance computer 'Colossus'.

2.2.2 Computational domain

The mesh for each case was created using OpenFOAM's meshing utility *blockMesh*. A slope of 3° preceded each dune shape for 50 m upwind and each dune profile was replicated as per figure 1 and extended uniformly breadthways for 160 m to account for any transverse flow which may occur particularly in lee of a dune (Jackson et al., 2013; Walker and Shugar, 2013). In total, each computational domain measured 100 m x 160 m x 40 m. The 40 m vertical extent of the domain was prescribed to ensure the top of the computational domain was at least 5 times greater than the height of the dune (Franke et al., 2007). The three computational domains comprised of

approximately 2.5 million hexahedra cells which gradually decreased in cell size from the top of the computational wall to the surface.

2.2.3 Computational Boundary Conditions

Incident flow from directly onshore (0°) to highly oblique onshore (67.5°), was simulated at 22.5° increments. Wind speed at the inlet boundary was defined as logarithmic using Richards and Hoxey (1993) profile equations for κ-ε turbulence models (Equation 1).

$$U(z) = (u^*/\kappa)\ln(\frac{z+z_0}{z_0}) \qquad \text{(Equation 1)}$$

Where U (z) is the wind speed at height z, u* is shear velocity, k is the Von Karman constant (0.4187) and z_0 is the surface roughness length. Turbulence kinetic energy (k) and energy dissipation (ε) were also simulated at the inlet boundary using conditions prescribed by Richards and Hoxey (1993) equations 2 and 3.

$$k = (u^*)^2/\sqrt{C_u} \qquad \text{(Equation 2)}$$

$$\varepsilon\,(z) = (u^*)^3/\kappa(z + z_0) \qquad \text{(Equation 3)}$$

where C_u is a constant of the k-ε model and equals 0.09. For all simulations and parameters, $u^*$was equivalent to 0.44 m s^{-1}, producing a wind speed of 8.00 m s^{-1} at 1 m above the surface at the inlet.

The surface of the beach and ridge/dyke was given a uniform roughness length (z_0) of 0.0005 m based upon a surface comprised sand grains (Bagnold, 1960). Symmetry boundary conditions were used at the lateral boundaries when incident flow was perpendicular to the beach scraped structures and a zero gradient patch type was implemented at the upper boundary to sustain an equilibrium boundary layer.

2.3. Predicted sediment transport

Sediment transport was modelled using a transport equation by Lettau and Lettau (1977) where:

$$q = C\sqrt{\frac{d}{D}}\frac{\rho}{g}(u_* - u_{*t})u_*^2 \qquad \text{(Equation 4)}$$

q is sediment flux in kg m^{-1} s^{-1},*C* is a constant of 4.2, d is grain size in mm, D is the reference grain diameter, 0.25 mm, ρ is air density in kg m^{-3} (1.2466 kg m^{-3}), g is gravity in m s^{-2}, u_* is shear velocity in m s^{-1} and u_{*t} is threshold shear velocity in m s^{-1} (in this case 0.23 m s^{-1}(which was just above observed transport threshold in Sherman et al., 1998)). Shear velocity (u_*) was calculated by:

$$u_* = \sqrt{(\frac{\tau}{\rho})} \qquad \text{(Equation 5)}$$

where τ is shear stress (m^2 s^2) calculated at the surface of the CFD model. This is distinctly different to the traditional technique of deriving shear stress from a regression of the vertical wind profile which limits the accuracy range up to +-20% on beaches (Sherman et al., 1998) and is only applicable where the vertical velocity profile is logarithmic.

Sediment transport was also corrected for the effect of surface slope, relative to the incident wind direction (Bagnold, 1973). Where slope adjusted transport (*q'*) is calculated by *Gq* where *G* is:

$$G = \frac{tan\alpha}{cos\theta(tan\alpha + tan\theta)} \qquad \text{(Equation 6)}$$

α is the angle of internal friction of the sediments (34°) and θ is the surface slope. Sediment grain size in each simulation case was classed as fine/medium with a diameter of 0.25 mm. Predicted sediment transport values are however only an estimate for coastal-aeolian environments (Sherman et al., 1998) and sediment transport in natural environments is chaotic and rarely, if ever, constant (Davidson-Arnott and Bauer, 2009). Furthermore many large wind events are also associated with rainfall which greatly limits actual sediment transport rates.

3. Results

3.1. Shear velocity and wind flow dynamics

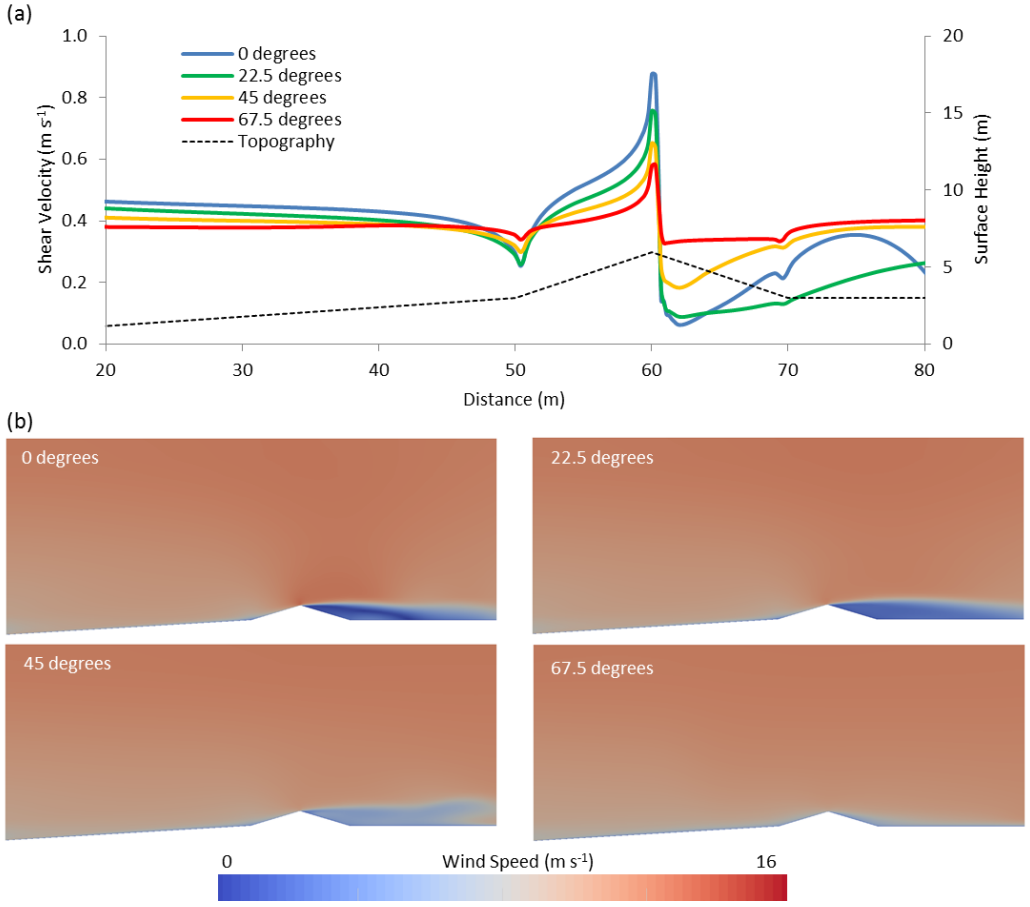

Figure 2. (a) Shear velocity (m s^{-1}) across the single ridge structure for four incident wind direction scenarios. Distance is relative to the westerly (left side) inlet boundary. Shear stress is highest at the crest and declines with increasing obliquity. (b) Two-dimensional slices (100m x 40m) of wind speed over the single ridge structure for the four incident wind direction scenarios. Deep blue indicates low wind velocity while red indicates high velocity. The velocity of wind flow at the crest of the structure decreases with increasing obliquity whilst wind velocity in lee of the structure increases.

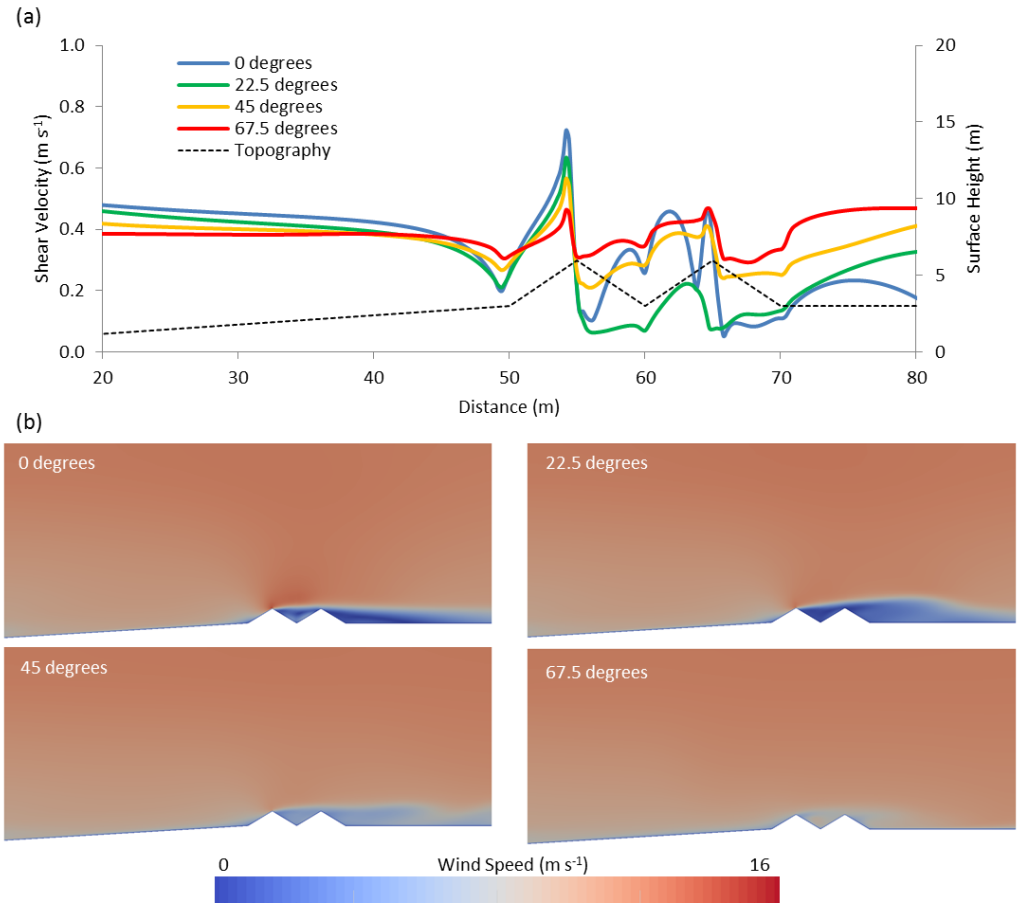

Figure 3. (a) Shear velocity (m s^{-1}) across the double ridge structure for four incident wind direction scenarios. Distance is relative to the westerly (left side) inlet boundary. (b) Two-dimensional slices (100m x 40m) of wind speed over the double ridge structure for the four incident wind direction scenarios. Deep blue indicates low wind velocity while red indicates high velocity. The velocity of wind flow at the crest of the structure decreases with increasing obliquity whilst wind velocity in lee of the structure increases.

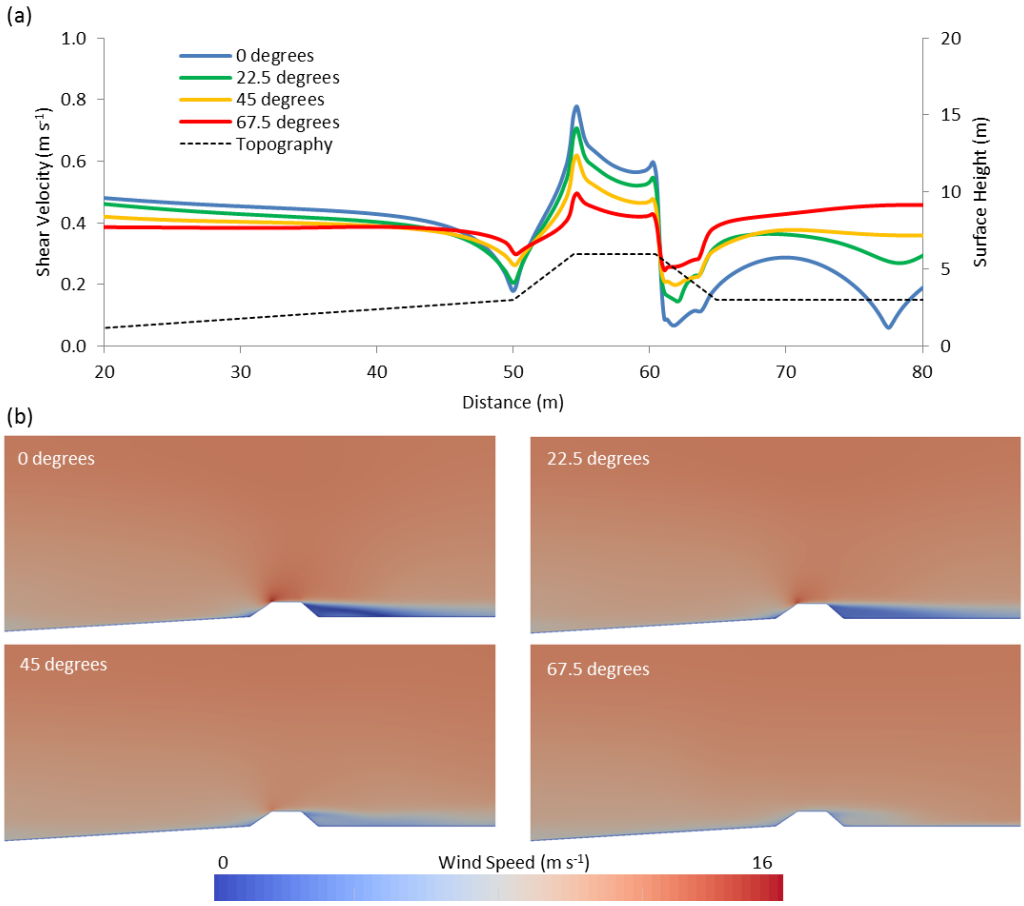

Figure 4. (a) Shear velocity (m s^{-1}) across the dyke ridge structure for four incident wind direction scenarios. Distance is relative to the westerly (left side) inlet boundary. (b) Two-dimensional slices (100m x 40m) of wind speed over the dyke structure for the four incident wind direction scenarios. Deep blue indicates low wind velocity while red indicates high velocity. The velocity of wind flow at the crest of the structure decreases with increasing obliquity whilst wind velocity in lee of the structure increases.

Shear velocity at the surface of each beach scraped structure is presented as a two dimensional transect and wind velocity as a two dimensional slice, 140 m north of the southern boundary in the computational domain (Figures 2-4). This location was selected to ensure the boundary layer had sufficiently developed. Figures 2-4 demonstrate that both shear velocity and wind speed on the beach upwind of the structure is uniform for each case and decreases incrementally with increasing angle of incident wind. As wind flow approaches the foot of the upwind slope, shear velocity and wind speed for all directions and structures is reduced, similar to data collected by Wiggs et al. (1996) in a wind tunnel. This reduction becomes smaller as incident wind direction becomes increasingly parallel to the crest. Shear velocity at the foot of the upwind slope is reduced the most by the dyke to a minimum of 0.18 m s^{-1} compared to 0.25 m s^{-1} and 0.30 m s^{-1} for the double and single ridge structures respectively. During 67.5° incident winds, flow at the toe of each structure increases to 0.31 m s^{-1} for both dyke and double ridge structures and 0.36 m s^{-1} for the single ridge.

On the stoss slope of each ridge/dyke scenario, shear velocity and wind speed increases with height before reaching a maximum at the crest of the structure. This value is greatest for the single ridge where shear velocity peaks at a maximum of 0.88 m s^{-1} during onshore flow. Shear velocity at the

crest of the double ridge and dyke are lower exhibiting values of 0.72 m s^{-1} and 0.78 m s^{-1} respectively. These peaks of shear velocity at the top of the stoss slope become smaller with increasingly oblique incident wind direction, reducing to 0.58 m s^{-1}, 0.46 m s^{-1} and 0.50m s^{-1} at the crest of the single ridge, double ridge and dyke respectively, for 67.5° winds.

In the lee of the ridge crests, each structure exhibited a different pattern of shear velocity and wind speed (Figures 2-4). Shear velocity in lee of the single ridge shape decreased abruptly, immediately downwind of the crest reaching a minimum of 0.06 m s^{-1} at the bottom of the lee slope (Figure 2a), before increasing within the separation envelope (Figure 2b) in lee of the ridge. As incident wind flow increased, the zone of flow separation diminishes (Figure 2b) and at 67.5°, little flow separation or flow retardation is appreciable (Figure 2b). A similar progression also occurred for the double ridge and dyke structures.

Shear velocity calculated in lee of the stoss slope of the double ridge exhibited the most complex pattern (Figure 3a). In resemblance to the single ridge, shear velocity rapidly decreased in the lee of the first crest for 0°winds however, this reduction became much less pronounced as wind direction relative to the crest increased. Wind speed also quickly recovered on the stoss slope of second crest, with the exception the 22.5° incident wind flow, during which wind speed remained low. At the crest of the secondary ridge, shear velocity is lower than that at the primary crest by 35% for 0° winds, 65% for 22.5° winds and 28% for 45° winds. Conversely shear velocity at the secondary crest for 67.5° winds increased by 2%.

Shear velocity across the top (or tread) of the dyke did not experience an abrupt decrease in shear velocity as observed in the single and double ridge examples (Figure 4a). Shear velocity on the flat top of the dyke, only decreased by a maximum of 28% compared to shear velocity at the break of slope between the stoss slope and tread. In similarity to the ridge examples, a distinct zone of wind flow separation and recirculation was created in lee of the structure (Figure 4b). Wind speed declined in lee of the structure to a minimum of 0.07 m s^{-1} for 0° winds and a minimum of 0.26 m s^{-1} for 67.5° winds. This increase in leeside wind speed with increasing incident wind direction obliquity, is exemplified in figure 4b.

3.2 *Sediment transport*

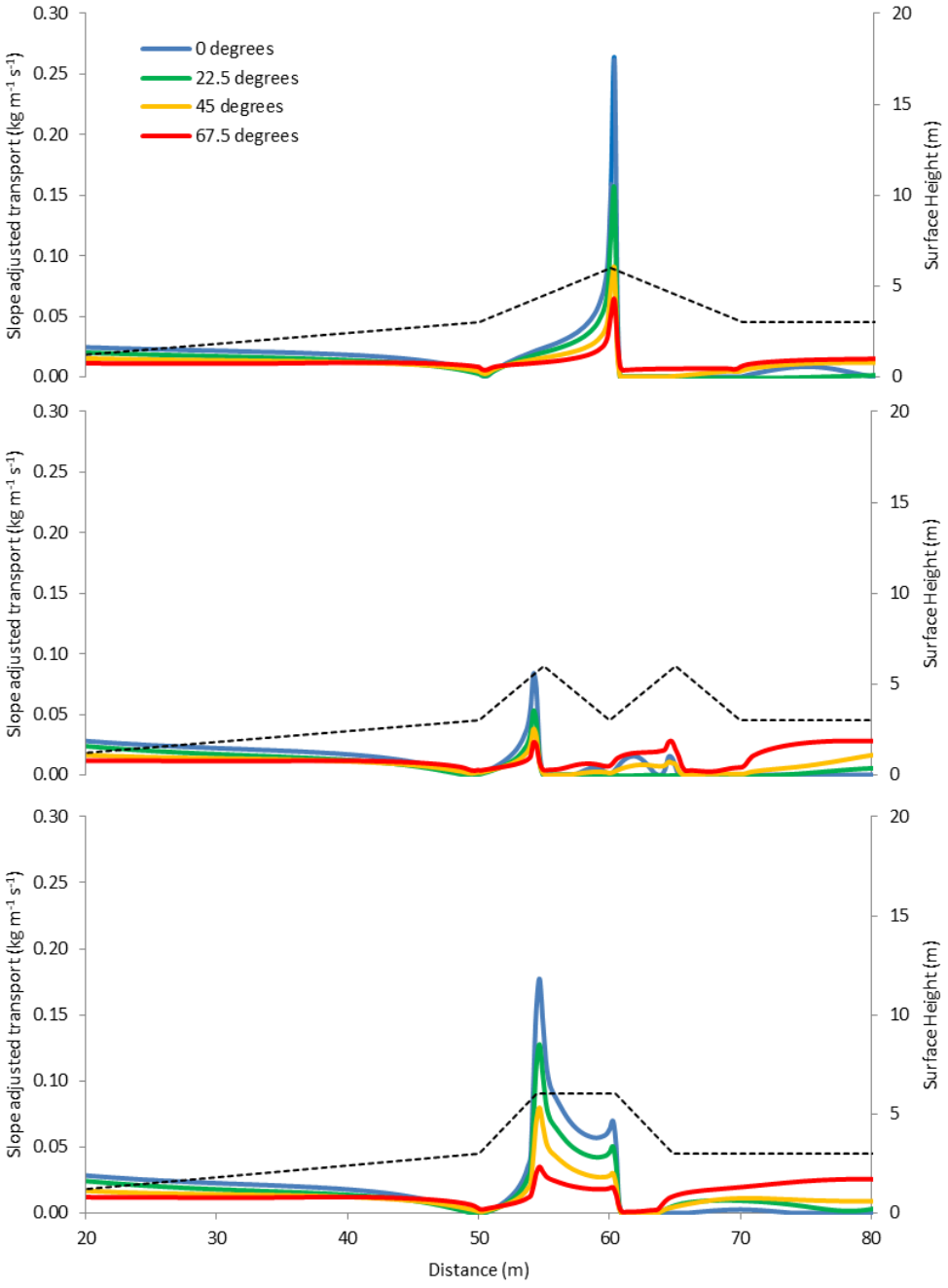

Figure 5. Slope adjusted sediment transport for the single ridge (a), double ridge (b) and dyke (c). Note in all cases sediment transport is greatest at the crest of the stoss slope for directly onshore winds (0°) but that sediment transport is greatest in the lee for 67.5° winds.

Sediment transport on each ridge/dyke shape was calculated over a two dimensional transect using an aeolian sand transport model developed by Lettau and Lettau (1977), hereby referred to as transport rate. In each case the transport rate on the beach was greatest for 0° winds and lowest for 67.5° winds. Transport rate was greatest at the crest for each wind direction and structure examined (Figure 5). The crest of the single ridge experienced the highest transport rate, followed by the dyke and double ridge. For all structures the transport rate on the beach, stoss slope and crest (including

the top of the dyke structure) decreased with increasing incident wind direction obliquity. In the lee of each structure however, the opposite is true. Here the transport rate became greater with increasing obliquity, with the transport rate in lee of the structure being approximately equal to that on the upwind beach surface, for each structure during 67.5° incident winds. Within the separation zone, created in the lee of each structure during 0°- 45° incident winds (Figures 2-4), some sediment transport does occur (Figure 5). Sediment transport occurring within this zone during 0° -45° winds is likely to be transported laterally or opposite to the incident wind direction as wind flow becomes deflected alongshore or separated, moving in the opposite bearing to that of the incident wind (Jackson et al., 2013; Walker and Shugar, 2013).

4. Discussion

The shape of dunes, ridges, berms and dykes created by beach scraping have to date been designed ad-hoc or at best using guidelines that take little consideration of aeolian sand transport or of natural foredune shapes and profiles (MacArthur et al., 2005; NSW Department of Land and Water Conservation, 2001). Although this study demonstrates wind flow patterns and shear velocity over three common scraped ridge/dyke forms during one incident wind speed, evidence from ultrasonic anemometry studies and CFD simulations over complex coastal dunes indicate that the patterns of flow steering, reversal and relative wind speed remain constant from fresh breeze to hurricane force winds (Hesp et al., 2005; Smyth et al., 2013), increasing the applicability of this study to a wide range of conditions.

The sediment transport rate at the crest of the single ridge was the greatest calculated in the study. Critically, high rates of sediment transport at the top of the stoss slope may allow sediment to be ejected beyond the crest, causing the formation of nuisance dunes in lee of the structure beyond the beach/dune expanse. The single ridges relatively low stoss slope angle (17°), also creates the smallest zone of wind speed and shear velocity retardation at the toe of the structure, minimising sediment deposition on the back beach and maintaining sediment transport from the beach to the stoss slope.

Overall, the greatest sediment transport rate was calculated over the topography of the dyke structure (Figure 5c). This structure appears to lack the resilience required to provide lasting protection from flooding and coastal inundation as the relatively wide flat top (tread) of the structure is exposed to topographically accelerated wind flow (Figure 4b), increasing the potential for sediment deflation, structure degradation and the formation of 'nuisance dunes' in lee of the structure. In addition, due to the steep slope of the dyke and the resulting reduction in shear velocity at the toe of the structure, sediment may accumulate at the toe of the dune where wind speed is insufficient to maintain transport. This accumulation upwind of the structure, will form a ramp that without regular sediment removal and maintenance will create a stoss slope comparable to the single dune (Christiansen and Davidson-Arnott, 1994), providing an aerodynamic ramp for further downwind sediment transport (Hesp et al., 2009).

The double ridge design exhibits the lowest values of sediment transport, both at the crest of the structure and over the length of the transect (Figure 5). This is due to the steep stoss slope and expansive zone of flow separation created between the ridges and downwind of the structure (Figure 3b). This large zone of flow separation permits sediment transported from the beach and stoss slope to be deposited immediately in lee of the stoss slope. This process the may be capable of

aiding the dune building process (Lynch et al., 2009). The double structures topographic heterogeneity is also advantageous for the development of a more diverse flora and fauna if vegetation is allowed or encouraged to grow or is planted (Acosta et al., 2009).

It should be noted that this study only represents wind flow and predicted sediment transport over the initial ridge and dyke structures. These shapes are susceptible to change with erosion and deposition of aeolian sediment, evolving into different morphologies over time. In the field all three structures are also vulnerable to wave attack during a storm event.

5. Link to Coastal Management Strategies

As aeolian geomorphologists the authors would always prefer to see a naturally functioning dune built on the backshore rather than an engineered ridge structure which barely replicates a natural dune shape. None of the shapes modelled replicate a natural foredune, least of all the dyke structure, and the dyke should never be referred to as a 'dune'. There are few, if any natural unmanaged foredunes in the world that resemble a banket, berm or dyke (Hesp and Walker, 2013). However, it is a common quick fix to build such structures particularly where infrastructure and communities are at risk following storms.

Of the three shapes examined, and as a rough guideline for management, the double ridge structure is the 'best' option of the three. While significant transport can occur on the foremost ridge, and the dune crest will lower over time if the ridge is not planted with vegetation, most of the sediment will be deposited in the inter-dune ridge swale. The double ridge structure has a significant lee flow separation or wake zone providing greater protection from the wind, and the least chance for nuisance (or leeward) dunes to develop downwind. Vegetation plantings would be better protected on the landward ridge in the initial stages of growth, and pioneer species would respond positively to the sedimentation taking place in the swale. A more diverse vegetation community would also be more likely to develop in the topographically more complex environment afforded by the two-ridge structure.

6. Conclusion

The findings of this study demonstrate that for each beach scraped structure examined, wind flow perpendicular to the crest of the structure undergoes the most wind flow acceleration and sediment transport. Winds oblique to the crest create a less steep relative slope (equation 6), but also less topographic acceleration resulting in a decrease in sediment transport. In lee of the structure however sediment transport becomes greater with increased obliquity as the extent of the separation zone decreases.

Based on the modelling conducted, this study recommends the construction of double ridges at sites where beach scraping is implemented, and beach width allows. Naturally, less morphological change will occur on all structures if they are planted immediately following construction.

7. Acknowledgements

The authors would like to acknowledge Robin Davidson-Arnott and an anonymous reviewer whose suggestions greatly improved the final manuscript. We also thank the School of the Environment, Faculty of Science and Engineering, Flinders University for funding and support.

8. References

Acosta, A., Carranza, M.L., Izzi, C.F., 2009. Are there habitats that contribute best to plant species diversity in coastal dunes? Biodiversity Conservation 18, 1087-1098.

Baas, A.C.W., 2002. Chaos , fractals and self-organization in coastal geomorphology : simulating dune landscapes in vegetated environments. Geomorphology 48, 309–328.

Bagnold, R.A., 1960. The physics of blown sand and desert dunes. Methuen and Co. Ltd, London.

Bagnold, R.A., 1973. The nature of saltation and 'bed-load' transport in water. Proc. R. Soc. London, Ser. A 332, 473-504

Bruun, P., 1983. Beach scraping - Is it damaging to beach stability? Coastal Engineering 7, 167–173.

Christiansen, M.B., Davidson-Arnott, R., 1994. Rates of landward sand transport over the foredune at Skallingen , Denmark and the role of dune ramps. Danish Journal of Geography 104, 31–43.

Conaway, C. A., Wells, J.T., 2005. Aeolian dynamics along scraped shorelines, Bogue Banks, North Carolina. Journal of Coastal Research 212, 242–254.

Cooke, B.C., Jones, A.R., Goodwin, I.D., Bishop, M.J., 2012. Nourishment practices on Australian sandy beaches: a review. Journal of Environmental Management 113, 319–27.

Davidson-Arnott, R. G. D., Bauer, B. O. 2009. Aeolian sediment transport on a beach: Thresholds, intermittency, and high frequency variability. Geomorphology 105(1-2), 117–126. doi:10.1016/j.geomorph.2008.02.018

Franke, J., Hellsten, A., Schlu¨nzen, H., Carissimo, B., 2007. Best practice guideline for the CFD simulation of flows in the urban environment. COST Action 732: Quality Assurance and Improvement of Microscale Meteorological Models

Gómez-Pina, G., Muñoz-Pérez, J.J., Ramírez, J.L., Ley, C., 2002. Sand dune management problems and techniques , Spain . Journal of Coastal Research 332, 325–332.

Hall, M.J., Pilkey, O.H., 1991. Effects of hard stabilization on dry beach width for New Jersey. Journal of Coastal Research 7, 3, 771-785.

Hesp, P., 2002. Foredunes and blowouts: initiation, geomorphology and dynamics. Geomorphology 48, 245–268.

Hesp, P.A., Walker, I.J., Davidson-Arnott, R.G., Ollerhead, J., 2005. Flow dynamics over a vegetated foredune at Prince Edward Island, Canada. Geomorphology 65, 71-84.

Hesp, P.A., Walker, I.J., Namikas, S.L., Bauer, B.O., Ollerhead, J., Allison, M., 2009. Storm Wind Flow over a Foredune , Prince Edward Island , Canada. Journal of Coastal Research 2009, 312–316.

Hesp, P.A. and I.J. Walker, 2013. Aeolian environments: coastal dunes. In: Shroder, J. (Editor in Chief), Lancaster, N., Sherman, D.J., Baas, A.C.W. (Eds.), Treatise on Geomorphology, vol. 11, Aeolian Geomorphology. Academic Press, San Diego, CA, pp. 109-133.

Hesp, P.A., Smyth, T.A.G., Nielsen, P., Walker, I.J., Bauer, B.O., Davidson-Arnott, R., *in press*. Flow deflection over a foredune. Geomorphology.

Hylgaard, T., Liddle, M.J., 1981. The effects of human trampling on a sand dune ecosystem dominated by empetrum nigrum. Journal of Applied Ecology 18, 2, 559-569

IPCC, 2012. Managing the risks of extreme events and disasters to advance climate change adaptation. A special report of working groups I and II of the intergovernmental panel on climate change [Field, C.B., V. Barros, T.F. Stocker, D. Qin, D.J. Dokken, K.L. Ebi, M.D. Mastrandrea, K.J. Mach, G.-K. Plattner, S.K. Allen, M. Tignor, and P.M. Midgley (eds.)]. Cambridge University Press, Cambridge, UK, and New York, NY, USA, 582 pp.

Jackson, D.W.T., Beyers, J.H.M., Lynch, K., Cooper, J. a. G., Baas, a. C.W., Delgado-Fernandez, I., 2011. Investigation of three-dimensional wind flow behaviour over coastal dune morphology under offshore winds using computational fluid dynamics (CFD) and ultrasonic anemometry. Earth Surface Processes and Landforms 36, 1113–1124. doi:10.1002/esp.2139

Jackson, D.W.T., Beyers, M., Delgado-Fernandez, I., Baas, A.C.W., Cooper, A.J., Lynch, K., 2013. Airflow reversal and alternating corkscrew vortices in foredune wake zones during perpendicular and oblique offshore winds. Geomorphology 187, 86–93.

Lettau, K., Lettau, H., 1977. Experimental and micrometeorologi- cal field studies of dune migration. In: Lettau, K., Lettau, H. (Eds.), Exploring the World's Driest Climate. University Wisconsin-Madison, IES Report 101, pp. 110-147.

Lynch, K., Jackson, D.W.T., Cooper, J.A.G., 2009. Foredune accretion under offshore winds. Geomorphology 105, 139–146. doi:10.1016/j.geomorph.2007.12.011

MacArthur, B., Coulton, P.E., Dean, B., Hatheway, D., Honeycutt, M., Johnson, J., Jones, C., Komar, P., Lu, C., Noble, R., Ruthven, T., Seymour, D., 2005. FEMA coastal flood hazard analysis and mapping guidelines focused study report. FEMA, February 2005.

Martínez, M.L., Gallego-Fernández, J.B., Hesp, P.A. (Eds.), 2013. Restoration of coastal dunes. Springer, Berlin.

Nichols, G.R., 1996. Preliminary observations on managing and reclaiming frontal dunes within the Durban municipal area. Landscape and Urban Planning 34, 383–388.

Nield, J.M., Baas, A.C.W., 2008. Investigating parabolic and nebkha dune formation using a cellular automaton modelling approach. Earth Surface Processes and Landforms 740, 724–740.

Nordstrom, K.F., Arens, S.M., 1998. The role of human actions in evolution and management of foredunes in The Netherlands and New Jersey , USA. Journal of Coastal Conservation 4, 169–180.

Nordstrom, K.F., Jackson, N.L., 2013. Foredune restoration in urban settings, in: Martínez, M.L., Gallego-Fernández, J.B., Hesp, P.A. (Eds.), Restoration of Coastal Dunes. Springer, Berlin.

NSW Department of Land and Water Conservation 2001, Coastal dune management: A manual of coastal dune management and rehabilitation techniques, Coastal Unit, DLWC, Newcastle.

Olff, H., Huisman, J., Van Tooren, B.F., 1993. Species dynamics and nutrient accumulation during early primary succession in coastal sand dunes. Journal of Ecology 81, 693–706.

Pattanapol, W., Wakes, S.J., Hilton, M.J., Dickinson, K.J.M., 2007. Modeling of Surface Roughness for Flow Over a Complex Vegetated Surface. Proceedings of world academy of science, Engineering and Technology 26, 273–281.

Petersen, C.H., Hickerson, C.H.M., Grissom Johnson, G., 2000. Short-Term consequences of nourishment and bulldozing on the dominant large invertebrates of a sandy beach. Journal of Coastal Research 16, 368-378.

Richards, P.J., Hoxey, R.P., 1993. Appropriate boundary conditions for computational wind engineering models using k-e turbulence model. Engineering and Industrial Aerodynamics 46, 145–153.

Sherman, D.J., Jackson, D.W.T., Namikas, S.L., Wang, J., 1998. Wind-blown sand on beaches : an evaluation of models. Geomorphology 22, 113–133.

Short, A.D., 1999. Wave-dominated beaches. In: A.D. Short (editor), Handbook of Beach and Shoreface Morphodynamics. J. Wiley and Sons, Chichester: 173-203

Smyth, T.A.G., Jackson, D.W.T., Cooper, J.A.G., 2012. Geomorphology High resolution measured and modelled three-dimensional airflow over a coastal bowl blowout. Geomorphology 177-178, 62-73.

Smyth, T.A.G., Jackson, D.W.T., Cooper, J.A.G., 2013. Three dimensional airflow patterns within a coastal trough – bowl blowout during fresh breeze to hurricane force winds, Aeolian Research 9, 111-123.

Versteeg, H.K., Malalasekera, W., 2006. An introduction to computational fluid dynamics, Second. ed. Pearson, Harlow.

Wakes, S.J., Maegli, T., Dickinson, K.J., Hilton, M.J., 2010. Numerical modelling of wind flow over a complex topography. Environmental Modelling & Software 25, 237–247.

Walker, I.J.,Shugar, D.J., 2013. Secondary wind flow deflection in the lee of transverse dunes with implications for dune morphodynamics and migration. Earth Surface Processes and Landforms 38, 1642-1654

Webster, P.J., Holland, G.J., Curry, J. a, Chang, H.-R., 2005. Changes in tropical cyclone number, duration, and intensity in a warming environment. Science (New York, N.Y.) 309, 1844–6.

Werner, B.T., 1995. Eolian dunes : Computer simulations and attractor interpretation. Geology 23, 1107–1110.

Whitehead, P.S., 1964. Sand dune reclamation in New Zealand. New Zealand Journal of Forestry, 9, 146-153

Wiggs, G.F.S., Livingstone, I., Warren, A., 1996. The role of streamline curvature in sand dune dynamics: evidence from field and wind tunnel measurements. Geomorphology 17, 29–46

Willis, C.M., Griggs, G.B., S., March, N., 2003. Reductions in fluvial sediment discharge by coastal dams in California and implications for beach sustainability. The Journal of Geology 111, 167–182.

Zheng, X. J., 2009. Mechanics of Wind-Blown Sand Movements. Springer, Berlin.

Zhang, D., Narteau, C., Rozier, O., Courrech du Pont, S., 2012. Morphology and dynamics of star dunes from numerical modelling. Nature Geoscience 5, 463–467.